Dominant role of greenhouse-gas forcing in the recovery of Sahel rainfall

Article

Accepted Version

Dong, B. ORCID: https://orcid.org/0000-0003-0809-7911 and Sutton, R. ORCID: https://orcid.org/0000-0001-8345-8583
(2015) Dominant role of greenhouse-gas forcing in the recovery of Sahel rainfall. Nature Climate Change, 5 (8). pp. 757-760. ISSN 1758-678X doi: 10.1038/nclimate2664
Available at https://centaur.reading.ac.uk/40372/

Dominant role of greenhouse gas forcing in the recovery of Sahel rainfall

Buwen Dong and Rowan Sutton*

National Centre for Atmospheric Science, Department of Meteorology, University of Reading

* Corresponding author: Rowan Sutton. E-mail: r.sutton@reading.ac.uk

Sahelian summer rainfall, controlled by the West African Monsoon (WAM), exhibited large amplitude multi-decadal variability during the twentieth century. Particularly important was the severe drought of the 1970s and 1980s, which had widespread impacts[1-6]. Research into the causes of this drought has identified anthropogenic aerosol forcing[3-4,8] and changes in sea surface temperatures (SSTs)[1-2,6,9-12] as the most important drivers. Since the 1980s, there has been some recovery of Sahel rainfall[2-7,12-14], although not to the pre-drought levels of the 1940s and 1950s. Here we report on experiments with the atmospheric component of a state-of-the-art climate model to identify the causes of this recovery. Our results suggest that the direct influence of higher levels of greenhouse gases in the atmosphere was the main cause, with an additional role for changes in anthropogenic aerosol precursor emissions. We find that recent changes in SSTs, although substantial, did not have a significant impact on the recovery. The simulated response to anthropogenic forcing is consistent with a multivariate fingerprint of the observed recovery, raising confidence in our findings. Whilst robust predictions are not yet possible, our results suggest that the recent recovery in Sahel rainfall is most likely to be sustained or amplified in the near term.

The Sahel drought of the 1970s and 1980s had devastating impacts on local populations and has been widely studied as one of the most important examples in instrumental records of changes in the hydrological climate of any region[1-6]. Between the 1950s and 1980s Sahelian summer rainfall declined by around 40%, associated with a spatially coherent pattern of rainfall change across most of North Africa[1-4]. Early studies on the causes of the drought focused on the role of the land surface[15] and changes in sea surface temperatures (SST) in the Atlantic[1-2,6,9-10,12] and Indian Ocean[11-12] basins. The relevant changes in SST may have arisen from natural internal variability or in response to changing forcings. More recent studies have explored the role of changing anthropogenic forcings, with several studies concluding that increases in anthropogenic aerosol precursor emissions from North America and Europe were a particularly important factor[3-4, 8]. One likely consequence of these aerosol precursor emissions was to cool SST in the North Atlantic Ocean relative to the South Atlantic, making a link with the previous research on the influence of SST changes.

Since the 1980s, the amounts of Sahel summer (July-August-September) rainfall have increased[2-7,12-14] (Figs 1a,b,& c and Supplementary Fig S1). The increase between the recent period 1996-2010/11 and the drought period 1964-1993 was 0.26 - 0.31 mm day^{-1} (estimated from three data sets), corresponding to around one third of the decrease that occurred between the 1950s and the drought period. The largest increases have occurred in August, which is climatologically the wettest month (Fig 1b). In view of the devastating impacts of the drought, understanding the reasons for this recent recovery, and whether it is likely to be sustained, is a key challenge.

The recovery in Sahel rainfall is associated with coherent changes in the regional climate: a warming of the African continent (Fig. 1d and Supplementary Fig S1) with an anomaly of 0.82 – 1.02^{o}C over North Africa (estimated from three data sets), which has enhanced the land-sea thermal contrast between North Africa and surrounding oceans[7,12-14] (Supplementary Fig S2) and enhanced the meridional temperature gradient over North African land (Supplementary Fig S3) an intensification and northward shift[13] of convection in the African Inter-tropical Convergence Zone (ITCZ), implied by observed trends in Outgoing Longwave Radiation[13], an increased easterly shear in the Sahel region, with stronger surface westerly winds (which supply moisture from the Atlantic Ocean) and a stronger and northward shifted African Easterly Jet (AEJ)[13,16,18] (Supplementary Figs S3 and S4). These changes all indicate an enhanced Western African monsoon (WAM) in the recent period relative to the drought period of 1964-1993.

Since the drought, several potential drivers of Sahel rainfall have changed. Sea surface temperatures have warmed, particularly in the North Atlantic and Indian Oceans (Supplementary Fig S2). Greenhouse gas concentrations have increased (changes between 1964-93 and 1996-2011 are: 11% increase in CO_2, 18% increase in CH_4, and 6% increase in N_2O), and there have been significant changes in anthropogenic aerosol precursor emissions, including a significant decline in sulphur dioxide emissions from Europe and North America and a significant increase from Asia (Supplementary Fig S2). To understand the relative importance of these factors we carried out numerical experiments with the atmospheric component of a state of the art global climate model (see Methods section).

When all three factors are changed, the model simulates an increase in Sahel rainfall of 0.23 mm day^{-1}, similar to the observed change of 0.26 - 0.31 mm day^{-1}. The pattern of change (Fig 1f) shows a coherent anomaly stretching across North Africa in the region of the ITCZ (Supplementary Fig S5), and is also similar to that observed. The increase in rainfall is associated with coherent changes in surface air temperature (SAT) and atmospheric circulation over North Africa that provide a multivariate fingerprint of the forced changes (Fig 2a). This fingerprint features: a warming of SAT and reduced sea level pressure (SLP) over North Africa; an enhanced meridional temperature gradient; and an increased easterly shear, associated with stronger surface westerly winds and a stronger and northward shifted African Easterly Jet (AEJ). These features are all consistent with the observed strengthening of the WAM.

When individual forcing factors are changed separately we find, perhaps surprisingly, that the substantial changes in SST (Supplementary Fig S2) have almost no impact on Sahel rainfall[1-2,6,12,16] (Figs 2b & 3a). The changes in SST cause warming of SAT over North Africa but this warming is relatively uniform so the changes in the meridional temperature gradient, zonal wind shear and surface westerlies (Figs 2b, 3b & c, and Supplementary Fig S6), that are linked to a change in the WAM, are very weak. By contrast, the multivariate signal of a strengthened WAM is almost entirely reproduced in our experiments in response to changes in anthropogenic forcing, with no changes in SST (Fig 3d & f). The direct response to the anthropogenic forcings exhibits a pronounced increase in the meridional temperature gradient over North Africa, in the easterly shear, and in the surface westerlies, which directly impacts the WAM, as captured by our multivariate fingerprint (Figs 2b, 3d, e & f and Supplementary Fig S6). Furthermore, most of the signal - 74% of the change in Sahel rainfall - is simulated in response to the increase in greenhouse gas forcing alone. If the responses to individual forcings combine linearly (discussed below), this implies the additional 26% of the change in Sahel rainfall is a response to the change in anthropogenic aerosol precursor emissions (Fig. 2b and Supplementary Fig S7). Thus our results clearly indicate that greenhouse gas forcing has been the dominant factor in the recent recovery of Sahel rainfall.

The results shown in Figs 1-3 are based on experiments which investigate the impact of changing radiative forcings in the presence of SSTs for the recent period. To further understand the role of different forcing factors we carried out additional experiments in which the radiative forcings were changed in the presence of SSTs for the earlier drought period (see Methods section and Supplementary Figs S8-S10). The results again show that the change in anthropogenic forcing leads to a robust strengthening of the WAM (Supplementary Figs S8 & S9). The magnitude of the precipitation response is approximately 25% weaker than in the presence of recent period SSTs, which indicates some sensitivity to the background state. We hypothesise that this sensitivity may be caused partly by a positive feedback between changes in temperature and water vapour over the Sahel[14]. Consistent with this hypothesis, we find that the change in greenhouse gas forcing causes a larger change in water vapour in the presence of recent period SSTs (Supplementary Fig S10). Supplementary Fig S9 demonstrates that, to a good approximation, the responses to individual forcings combine linearly: there is evidence of small departures from linearity, but these departures are not statistically significant. Further investigation into the dependence on the background climate state of the WAM response to radiative forcing, and potential non-linear interactions between the responses to different forcings, is an important area for future research.

Our conclusions differ from some earlier studies[2,12], which suggested that warming of the subtropical North Atlantic SST was the primary cause of the recovery in Sahel rainfall. However, the model experiments reported in these studies showed changes in Sahel rainfall in response to Atlantic SST that were much weaker and noisier than the observed changes. Moreover these studies did not investigate the direct impact of changes in radiative forcings, which our results show to be dominant. We note that the response to the observed SST changes may exhibit some model dependence; investigating the extent of any such dependence would be a valuable area for future work.

Other previous studies have highlighted the importance of greenhouse gas forcing for Sahel rainfall in the *late* 21st century[5,7,16], and the mechanism identified in these studies is very similar to that we find. However, it is surprising that the much smaller (though still substantial) changes in greenhouse gases over recent decades nevertheless appear to have been large enough to control the evolution of such

an important feature of continental-scale climate as the WAM. Looking forward to the next few decades, greenhouse gas concentrations will continue to rise. Our results suggest that this rise is favorable for sustaining, and potentially amplifying, the recovery of Sahel rainfall. It is also expected that anthropogenic aerosol precursor emissions will decline globally. Large regional variations in emissions mean the impact of this decline is hard to anticipate in detail, but our results suggest that the impact on Sahel rainfall may be less important than that caused by the sustained increase in greenhouse gases. However, different patterns of SST change – arising from a combination of natural internal variability and forced responses – could well play a more important role in the future than in the recent past.

It will be important to repeat our study with other climate models, including at higher resolution and with explicit representation of ocean-atmosphere coupling. This work is urgent because the future of Sahel rainfall is a central concern for the drought-vulnerable populations of the region. There could also be important impacts on regions and peoples outside Africa. For example, a further enhancement of the zonal wind shear associated with Sahel rainfall could influence African Easterly Wave (AEW) intensity[18]. AEWs have been found to play a role in mobilizing and transporting Saharan dust across Africa and much further afield[20], and in initiating tropical cyclones in the Atlantic basin[21].

Methods

Observational data sets. The monthly mean SAT & precipitation data sets used are University of Delaware (UD) land SAT & precipitation v3.01 (1901-2010), CRU TS3.21 SAT & precipitation[22] (1901-2013) on a 0.5^{o}x0.5^{o} grid, the NOAA's Precipitation Reconstruction over Land (PREC/L) (1948-2013) on a 1^{o} x 1^{o} grid, GPCP v2.2 precipitation[23] (1979-2013) on a 2.5^{o} x 2.5^{o} grid, and the NASA GISS Surface Temperature Analysis[24] (GISTEMP)(1880-2013) on a 2^{o} x 2^{o} grid. Monthly mean SST from 1871 to 2013 is HadISST[25] on a 1^{o} x 1^{o} grid. Monthly mean variables of NCEP/NCAR reanalysis 2[26] (1979-2013) and monthly SLP of the 20th Century (20C) Reanalysis[27] v2 (1871-2012) are used. UD, PREC/L, GPCP, GISTEMP, NCEP/NCAR reanalysis 2 and the 20C reanalysis are provided by the NOAA/OAR/ESRL PSD, Boulder, Colorado, USA, from their Web site at http://www.esrl.noaa.gov/psd/. CRUTS3.21 data are available from the British Atmospheric Data Centre from the site http://badc.nerc.ac.uk/browse/badc/cru/data/cru_ts/cru_ts_3.21/data/. HadISST data are available from http://www.metoffice.gov.uk/hadobs/. The NCEP/NCAR reanalysis 2 is used to examine changes in the free troposphere since it uses an updated forecast model and data assimilation system and covers the satellite period of 1979 to the present[27]. Changes are analysed between a base period, 1964-93, during which the major Sahel drought occurred, and a recent period, 1996-2010/2011 (depending on dataset) during which Sahel rainfall had shown a significant recovery (Fig 1). In the case of the NCEP/NCAR reanalysis 2 data, a modified base period of 1979-1993 was used. Comparison of Fig 1e with Supplementary Fig S1 shows that a) the change in base period does not have a major impact on the pattern of SLP change seen in the 20C data, and b) the pattern of change in SLP is consistent between 20C and NCEP/NCAR reanalysis 2.

General circulation model. Climate model experiments have been carried out to identify the roles of changes in SST/Sea Ice extent (SIE), anthropogenic greenhouse gases (GHG) and anthropogenic aerosol (AA) forcing in the recent Sahel rainfall recovery. The model used is the atmosphere configuration of the Met Office Hadley Centre Global Environment Model version 3 (HadGEM3-A[28]), with a resolution of 1.875° longitude by 1.25° latitude and 85 levels in the vertical. The model includes an interactive

tropospheric chemistry scheme and five species (sulphate, black carbon, organic carbon, sea-salt, and dust) of tropospheric aerosols considering the aerosol direct, indirect, and semi-direct effects. Data sets required by the model for tropospheric aerosol scheme are emissions of sulphur dioxide (SO_2), land-based dimethyl sulphide (DMS), ammonia (NH_3), and primary black and organic carbon aerosols from fossil fuel combustion and biomass burning. Six numerical experiments have been performed (see details in Supplementary Table S1). They are: CONTROL forced by drought period SST/SIE, GHG and AA; ALL forced by recent period SST/SIE, GHG and AA; SSTGHG forced by recent period SST/SIE and GHG, but drought period AA; SSTONLY forced by recent period SST/SIE, but drought period GHG and AA; GHGAA forced by recent period GHG and AA, but drought period SST/SIE; and GHGONLY forced by recent period GHG, but drought period SST/SIE and AA. The last 25 years of each experiment are used for analysis and the response to a particular forcing is estimated by the mean difference between a pair of experiments that include and exclude that forcing. Seasonal mean values for summer (July-September, JAS) are produced by averaging corresponding monthly mean values. Statistical significance of the summer mean changes and the 5-95% confidence intervals of the mean changes in both observations and model experiments are assessed using a two tailed Student t-test.

Model climatology. The spatial patterns of the climatology in observations and in the model CONTROL experiment are shown in Supplementary Fig S5 and some WAM indices are in Supplementary Fig S4. The main features of the large scale circulation and precipitation are reproduced reasonably well in comparison with observations and reanalysis. The position of the Saharan heat low and its strength also compare well with observations. Associated with the Saharan heat low are strong southwesterly monsoon winds around ~10^{o}N, to the south of the heat low, and northeasterly winds to the north in observations. The model simulates the northeasterlies to the north of the heat low well, but underestimates the southwesterlies to the south. As the result, the model simulated precipitation does not extend northward enough, with mean Sahel rainfall being underestimated. It is likely that these biases are related to weaknesses in the representation of convection[29]. The underestimation of Sahel rainfall in the model is associated with a cold bias in SAT and a relatively weak meridional temperature gradient over North

Africa, linked to weak vertical shear of zonal wind, weak AEJ, and weak surface westerly winds over the Sahel (Supplementary Figs S3-S5). When comparing observations with model results the model results are adjusted to remove the mean biases, as shown in Supplementary Fig S4.

References

1. Folland, C. K., Palmer, T. N. & Parker, D. E. Sahel rainfall and worldwide sea temperatures, 1901–85. *Nature* **320**, 602-607 (1986).

2. Giannini A., Saravanan, R. & Chang, P. Oceanic forcing of Sahel rainfall on interannual to interdecadal time scales. *Science*, **302**, 1027–1030 (2003).

3. Held, I. M., Delworth, T. L., Lu, J., Findell, K. L. & Knutson, T. R. Simulation of Sahel drought in the 20th and 21st centuries. *Proc. Natl Acad. Sci.* **102**, 17891–17896 (2005).

4. Biasutti, M. & and Giannini, A. Robust Sahel drying in response to late 20th century forcings *Geophys. Res. Lett.* **33**, L11706 (2006).

5. Biasutti, M. Forced Sahel rainfall trends in the CMIP5 archive. *J. Geophys. Res. Atmos.* **118,** 1613–1623, doi:10.1002/jgrd.50206 (2013).

6. Giannini, A., Salack, S., Lodoun, T., Ali, A., Gaye, A. & Ndiaye, O. A unifying view of climate change in the Sahel linking intra-seasonal, interannual and longer time scales, *Environ. Res. Lett*. **8**, 024010, doi:10.1088/1748-9326/8/2/024010 (2013).

7. Haarsma, R. J., Selten, F., Weber, N. & and Kliphuis, M. Sahel rainfall variability and response to greenhouse warming. *Geophys. Res. Lett.*, 32, L17702, doi:10.1029/2005GL023232 (2005).

8. Ackerley, D. *et al.* Sensitivity of twentieth-century Sahel rainfall to sulphate aerosol and CO_2 forcing. *J. Climate*, **24**, 4999-5014 (2011).

9. Zhang, R. & Delworth, T. L. Impact of Atlantic multidecadal oscillations on India/Sahel rainfall and Atlantic hurricanes. *Geophys. Res. Lett.* **33**, L17712, doi:10.1029/2006GL026267 (2006).

10. Martin, E. R., Thorncroft, C. & Booth, B.B.B. The Multidecadal Atlantic SST - Sahel rainfall teleconnection in CMIP5 simulations. *J. Climate*, **27**, 784-806 doi: http://dx.doi.org/10.1175/JCLI-D-13-00242.1 (2014)

11. Bader, J. & Latif, M. The impact of decadal-scale Indian Ocean sea surface temperature anomalies on Sahelian rainfall and the North Atlantic Oscillation. *Geophys. Res. Lett.,* **30**, 2169. doi:10.1029/2003GL018426 (2003).

12. Hagos, S. M. & Cook, K. H. Ocean warming and late-twentieth-century Sahel drought and recovery. *J. Climate*, **21**, 3797–3814. doi: http://dx.doi.org/10.1175/2008JCLI2055.1 (2008).

13. Fontaine, B., Roucou, P. Gaetani, M. & Marteau, R. Recent changes in precipitations, ITCZ convection and northern tropical circulation over North Africa (1979-2007). *Int. J. Climatol.,* **31**, 633–648 (2011).

14. Evan, A. T. *et al*. Water vapor–forced greenhouse warming over the Sahara desert and the recent recovery from the Sahelian drought. J. Climate, 28, 108–123. doi: http://dx.doi.org/10.1175/JCLI-D-14-00039.1 (2015)

15. Charney J. G. Dynamics of deserts and drought in Sahel. *Quart. J. Roy. Meteor. Soc.*, **101**, 193–202 (1975).

16. Skinner, C. B., Ashfaq, M. & Diffenbaugh, N. S. Influence of twenty-first-century atmospheric and sea surface temperature forcing on west African Climate. *J. Climate*, **25**, 527–542 (2012).

17. Giannini, A. Mechanisms of climate change in the semiarid African Sahel: the local view. *J. Climate,* **23**, 743–756 (2010).

18. Skinner, C. B., & Diffenbaugh, N. S. Projected changes in African easterly wave intensity and track in response to greenhouse forcing. *Proc. Natl Acad. Sci*, **111**, 6882-6887 (2014).

19. Roehrig R. D. et al. The present and future of the West African monsoon: a process-oriented assessment of CMIP5 simulations along the AMMA transect. J. Climate. 26, 1–88 (2013).

20. Knippertz, P. & Todd, M. C. The central west Saharan dust hot spot and its relation to African easterly waves and extratropical disturbances. *J. Geophys. Res.,* **115**, D12117 (2010).

21. Hopsch, S. B., Thorncroft, C. D. & Tyle, K. R. Analysis of African easterly wave structures and their role in influencing tropical cyclogenesis. *Mon. Weather Rev.,* **138**, 1399–1419 (2010).

22. Harris, I., Jones, P.D., Osborn, T.J., & Lister, D.H. Updated high-resolution grids of monthly climatic observations – the CRU TS3.10 Dataset, *Int. J. Climatology*, **34**, 623-642, Doi: 10.1002/joc.3711 (2014).

23. Adler, R.F. *et al*. The Version 2 Global Precipitation Climatology Project (GPCP) Monthly Precipitation Analysis (1979-Present). J. Hydrometeor. **4**, 1147–1167 (2003)**.**

24. Hansen, J., Ruedy, R. Sato, M. & Lo, K. Global surface temperature change, *Rev. Geophys.*, **48**, RG4004, doi:10.1029/2010RG000345 (2010).

25. Rayner, N. A. *et al*. Global analyses of sea surface temperature, sea ice, and night marine air temperature since the late nineteenth century J. Geophys. Res. **108**, D14, 4407 doi:10.1029/2002JD002670 (2003).

26. Kanamitsu, M. *et al.* NCEP–DOE AMIP-II Reanalysis (R-2). *Bull. Amer. Meteor. Soc.*, **83**, 1631–1643. doi: http://dx.doi.org/10.1175/BAMS-83-11-1631 (2002).

27. Compo, G.P. *et al*. The Twentieth Century Reanalysis Project. *Quarterly J. Roy. Meteorol. Soc*., **137**, 1-28. DOI: 10.1002/qj.776 (2011).

28. Hewitt, H. T. *et al*. Design and implementation of the infrastructure of HadGEM3: The next-generation Met Office climate modelling system. *Geosci. Model Dev*., **4**, 223–253 (2011).

29. Birch, C. E. *et al*. A seamless assessment of the role of convection in the water cycle of the West African Monsoon. *J. Geophys. Res. Atmos.*, **119**, 2890–2912, doi:10.1002/ 2013JD020887 (2014).

30. Lamarque, J.-F. *et al*. Historical (1850–2000) gridded anthropogenic and biomass burning emissions of reactive gases and aerosols: Methodology and application. *Atmos. Chem. Phys.*, **10**, 7017–7039 (2010).

Acknowledgments

This work was supported by the PAGODA project of the Changing Water Cycle programme of UK Natural Environment Research Council (NERC) under grant NE/I006672/1 and the European Union's

Seventh Framework Programme [FP7/2007-2013] under grant agreement no 607085. BD and RS are also supported by the UK National Centre for Atmospheric Science, funded by the Natural Environment Research Council. The authors would like to thank Dr Alessandra Giannini for helpful comments.

Author contributions

BD and RS designed research. BD carried out experiments and analyses. BD and RS worked together on the interpretation of results and wrote the paper.

Additional information

Correspondence and requests for materials should be addressed to RS (r.sutton@reading.ac.uk)

Competing financial interests

The authors declare no competing financial interests.

Figure Legends

Figure 1: The recent recovery in Sahel rainfall: observed changes and model simulated responses. **a,** Time series of Sahel rainfall (mm day^{-1}) in July-September (JAS) over the land area (10^{o}-20^{o}N, 20^{o}W-35^{o}E) from three observational data sets. **b,** Seasonal evolutions of precipitation change (mm day^{-1}) between the recent period of 1996-2010/11 and the earlier period of 1964-1993, in observations and model simulations. **c-e,** Spatial patterns of observed seasonal mean (JAS) changes between the two periods in precipitation (mm day^{-1}), SAT (^{o}C), and SLP (hPa). The recent period for University of Delaware (UD) data sets is 1996-2010 and for the other datasets is 1996-2011. **f-h,** The same as in **c-e,** but the changes in the model simulated responses forced by changes in SST/SIE, GHG concentrations, and AA precursor emissions (ALL–CONTROL). Thick lines in **f and g** highlight regions where the differences are statistically significant at the 90% confidence level using a two-tailed Student t-test. Red and black boxes indicate the regions used to calculate some area (land only) averaged monsoon indices which are shown in Figure 2 and Supplementary Figures S4 and S9. See Methods for details of data sets and model experiments and analysis.

Figure 2: Observed and model simulated seasonal mean (July-September) changes in Sahel rainfall and related variables. a, Observed changes and simulated responses to changes in SST/SIE, GHG concentrations, and AA precursor emissions (ALL–CONTROL) for precipitation (mm day^{-1}) averaged over the Sahel (region shown by box in Fig 1f), SAT (^{o}C), and SLP (hPa) averaged over North Africa (region shown by box in Fig 1g), vertical zonal wind shear (m s^{-1}) between 925hPa and 600 hPa over the Sahel, African Easterly Jet (AEJ, m s^{-1}), defined as area averaged zonal wind at 600 hPa over the Sahel, and zonal wind (m s^{-1}) at 850 hPa over the Sahel. Observed anomalies are (1996-2010) minus (1964-1993) for precipitation and SAT based on University of Delaware data sets. SLP change are (1996-2011) minus (1964-1993) based on the 20^{th} century reanalysis. Zonal wind shear and zonal wind changes are (1996-2011) minus (1979-1993) based on NCEP reanalysis 2. The coloured bars indicated the central estimates and the whiskers show the 5-95% confidence intervals of the seasonal mean changes in both observations and model experiments based on a two tailed Student t-test. **b,** Model simulated changes in

monsoon indices in response to different forcings, normalized by the corresponding total response to all forcings (ALL–CONTROL). SST & SIE is the response to changes in SST/SIE (SSTONLY–CONTROL). GHG is the response to GHG concentrations (SSTGHG–SSTONLY), and AA is the response to changes in AA precursor emissions (ALL–SSTGHG). See Methods for details of data sets and model experiments, and analysis.

Figure 3: Spatial patterns of model simulated seasonal mean (July-September) changes in response to different forcings. a-c, Seasonal mean (JAS) changes in precipitation (mm day^{-1}), SAT (^{o}C), SLP (hPa) and 850 hPa wind (m s^{-1}) in response to changes in SST/SIE (SSTONLY–CONTROL). **d-f,** The same as in **a-c,** but for the responses to the changes in GHG concentrations, and AA precursor emissions (ALL–SSTONLY) . **g-i,** The same as in **a-c,** but for the responses to the changes in GHG concentrations (SSTGHG–SSTONLY). Thick lines highlight regions where the differences are statistically significant at the 90% confidence level using a two-tailed Student t-test. See Methods for details of data sets and model experiments, and analysis.

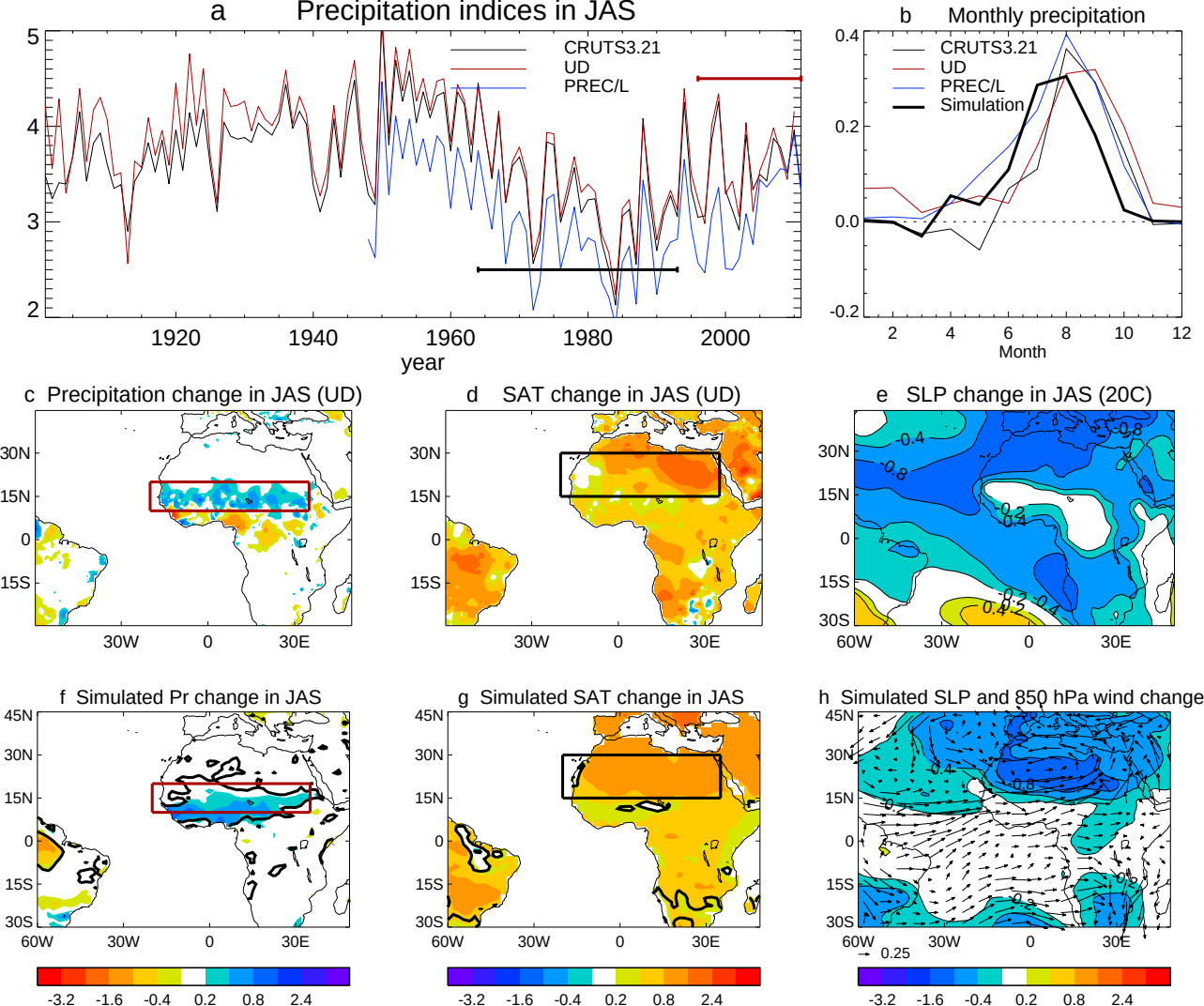
a Precipitation indices in JAS
CRUTS3.21
UD
PREC/L
year
b Monthly precipitation
CRUTS3.21
UD
PREC/L
Simulation
Month
c Precipitation change in JAS (UD)
d SAT change in JAS (UD)
e SLP change in JAS (20C)
f Simulated Pr change in JAS
g Simulated SAT change in JAS
h Simulated SLP and 850 hPa wind change
0.25
-3.2 -1.6 -0.4 0.2 0.8 2.4

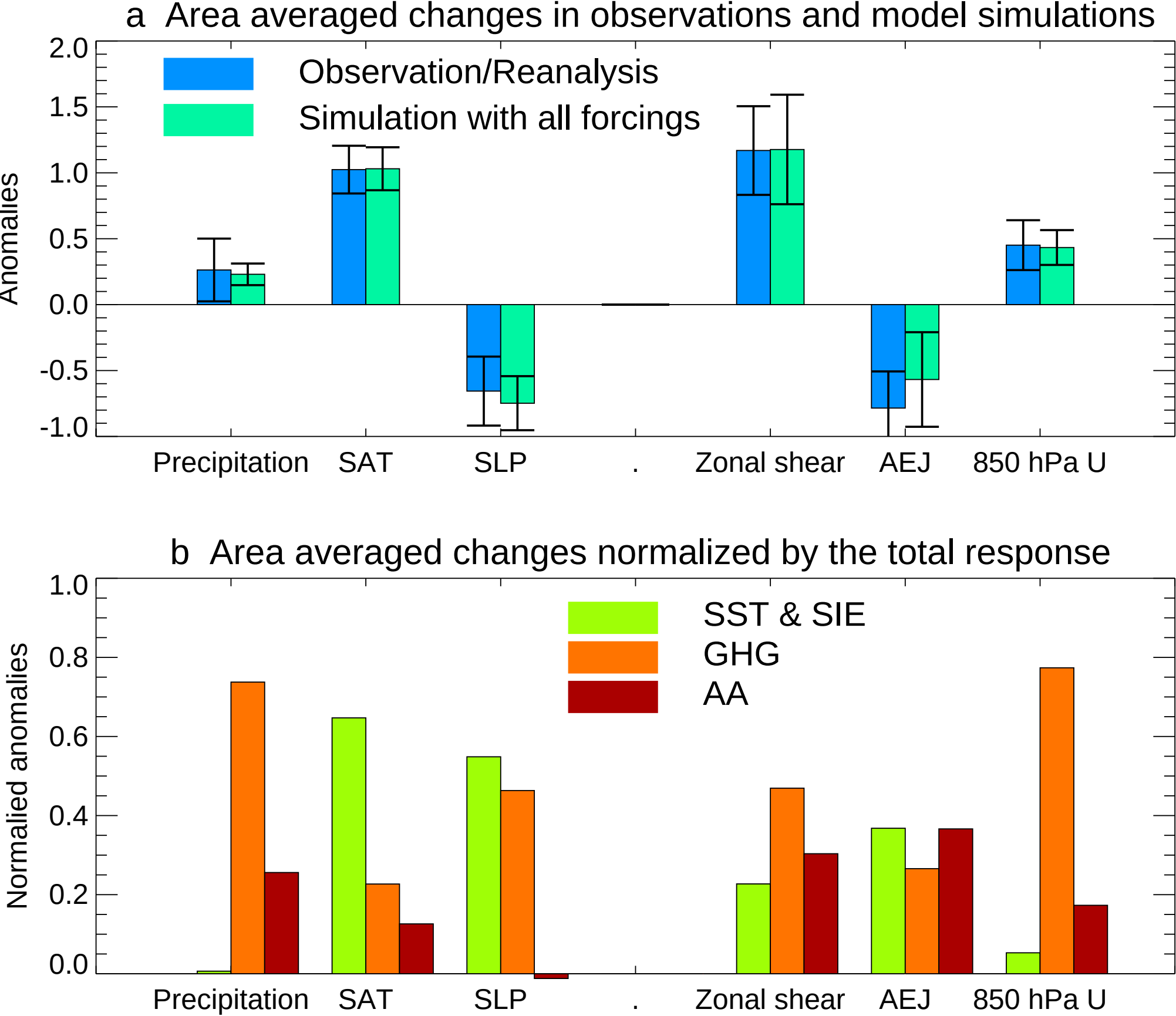
a Area averaged changes in observations and model simulations
Observation/Reanalysis
Simulation with all forcings
Anomalies
2.0
1.5
1.0
0.5
0.0
-0.5
-1.0
Precipitation
SAT
SLP
.
Zonal shear
AEJ
850 hPa U
b Area averaged changes normalized by the total response
SST & SIE
GHG
AA
Normalied anomalies
1.0
0.8
0.6
0.4
0.2
0.0
Precipitation
SAT
SLP
.
Zonal shear
AEJ
850 hPa U

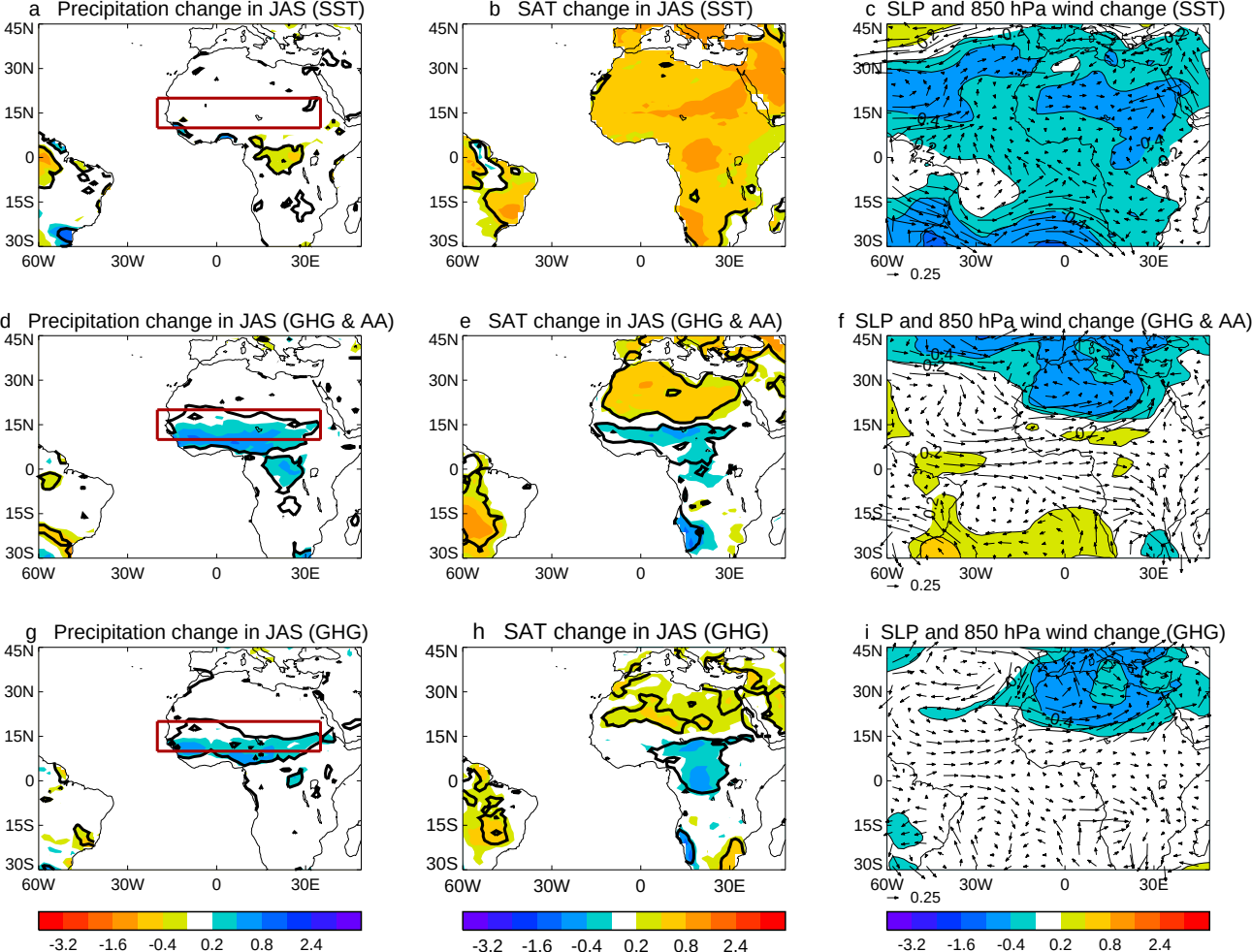
a Precipitation change in JAS (SST)
b SAT change in JAS (SST)
c SLP and 850 hPa wind change (SST)
d Precipitation change in JAS (GHG & AA)
e SAT change in JAS (GHG & AA)
f SLP and 850 hPa wind change (GHG & AA)
g Precipitation change in JAS (GHG)
h SAT change in JAS (GHG)
i SLP and 850 hPa wind change (GHG)
45N
30N
15N
0
15S
30S
60W
30W
0
30E
0.25
-3.2 -1.6 -0.4 0.2 0.8 2.4